Iraqi Journal of Science, 2026, Vol. 67, No. 2, pp: 629-640
DOI: 10.24996/ijs.2026.67.2.5

ISSN: 0067-2904

# Modified Carbon Nanofibers CNFs from Electrospun Polyacrylonitrile and Carbon Nanotubes PAN/CNTs

**Fatima M. Yahya[1]*, Manar A. Najim[1], Mohammed S. Hamza[2]**
[1]*Department of Materials Engineering, University of Technology-Iraq, Baghdad, Ira*
[2]*Department of Bio Medical Engineering, College of Engineering, Al-Esraa University, Baghdad, Iraq*

Received: 10/11/2024 Accepted: 6/9/2025 Published: 28/2/2026

**Abstract**

This study introduces a method to enhance the graphitization of carbon nanofiber (CNFs) by incorporating multi walled carbon nanotubes (MWCNTs) to polyacrylonitrile (PAN) as precursors to improve graphitization compared to CNFs produced from pure PAN precursors. Both traditional CNFs and modified CNFs/CNTs were synthesized via electrospinning followed by thermal treatment (stabilization at 275°C and carbonization at 1000°C in $N_2$ gas atmosphere). FE-SEM analysis showed a reduction in average fiber diameter after the addition of MWCNTs. Post-carbonization, the composite CNFs/CNTs exhibited a smaller diameter reduction (−13.54%) compared to pure CNFs (−25.05%), indicating enhanced structural stability. FTIR spectroscopy confirmed the effectiveness of adding MWCNTs to the graphitization process. XRD analysis revealed the successful carbonization of both CNFs and CNFs/CNTs specimens at 1000°C while Raman spectroscopy showed a slight decrease in $I_D/I_G$ intensity ratio from 1.22 for CNFs to 1.15 for CNFs/CNTs. Both the electrical conductivity and water contact angle were enhanced in the modified CNFs/CNTs compared with the traditional CNFs.

**Keywords:** Carbon nanofibers; Polyacrylonitrile; Stabilization; Carbonization; Electrospinning.

# الياف الكاربون النانوية المعدلةCNFs والمصنعة من البولي اكريلونترايل وانابيب الكاربون النانوية PAN/CNTs بطريقة البرم الكهربائي

**فاطمة يحيى[1]*،منار نجم[1]، محمد حمزة[2]**
[1] قسم هندسة المواد، الجامعة التكنولوجية ، العراق، بغداد، العراق
[2] قسم هندسة الطب الحياتي، كلية الهندسة، جامعة الإسراء، بغداد، العراق

**الخلاصة**

تُقدم هذه الدراسة طريقة لتحسين تبلور الياف الكاربون النانوية من خلال إضافة انابيب الكاربون النانوية متعددة الطبقات الى البولي اكريلونترايل كمادة أساس بهدف تحسين التبلور مقارنةً بالألياف المنتجة من البولي اكريلونترايل النقي. تم تصنيع كل من الياف الكاربون النانوية التقليدية والياف الكاربون النانوية المعدلة

*Email: mae.22.012@grad.uotechnology.edu.iq

باستخدام تقنية الغزل الكهربائي يتبعها معالجة حرارية (التثبيت بدرجة حرارة 275°م والكربنة بدرجة حرارة 1000°م وبوجود غاز النتروجين). أظهر تحليل المجهر الإلكتروني الماسح انخفاضًا في متوسط قطر الألياف بعد إضافة انابيب الكاربون النانوية. وبعد عملية الكربنة، أظهرت الألياف المركبة انخفاضًا أقل في القطر بنسبة −13.54% مقارنةً بالألياف النقية التي انخفض قطرها بنسبة −25.05%، مما يدل على تحسن في الاستقرار البنيوي. أكدت مطيافية الأشعة تحت الحمراء فعالية إضافة فعالية إضافة انابيب الكاربون النانوية في زيادة محتوى الكرافيت في الياف الكاربون النانوية المعدلة، كما اظهرت تحليل حيود الأشعة السينية كفاءة عملية الكربنة عند درجة حرارة 1000 °م. أظهرت مطيافية رامان انخفاضاً قليلاً في نسبة $I_D/I_G$ من 1.22 لألياف الكاربون النانوية التقليدية الى 1.15 لألياف الكاربون النانوية المعدلة كل من التوصيلية الكهربائية وقابلية التبلل تحسنتا في الياف الكاربون النانوية المعدلة مقارنة بألياف الكاربون النانوية التقليدية.

## 1. Introduction

One-dimensional 1D carbon nanofiber CNFs are highly regarded among low-dimensional carbon nanostructures because of their straightforward manufacturing process, exceptional chemical stability, ability to tolerate high temperatures, mechanical capabilities, and relatively good electrical conductivity [1]. Owing to their distinct structure, performance, and features, CNFs have shown promise in various fields, such as materials science, environmental science, tissue engineering, biomedicine, energy storage, and nanotechnology [2]. Polyacrylonitrile (PAN) is a common precursor for CNFs due to its environmental benefits, ease of dehydrocyclization, rapid pyrolysis rate, and high carbon yield [3]. Chemical vapor deposition (CVD) is the traditional technique employed to produce CNFs. CVD is well-known for its complexity and high cost. Consequently, a straightforward, cost-efficient electrospinning process has been progressively employed as the most effective technique for producing continuous CNFs [4, 5]. The subsequent heat treatments, which involve stabilization and carbonization processes, transform PAN precursor nanofibers into CNFs [6]. The stabilization step was carried out in an oxidative atmosphere at temperatures ranging from 200 °C to 300 °C. This stage is crucial for preventing the fusion of precursor nanofibers, minimizing volatilization, and optimizing the carbon yield during carbonization [4, 7]. A thermally stable infusible ladder structure is formed through chemical reactions that occur during the stabilization process, including cyclization, dehydrogenation, aromatization, oxidation, and cross-linking, which convert C≡N bonds to C=N bonds [8]. During the carbonization process, an inert gas such as argon or nitrogen is used to prevent the disintegration of the polymer chain [9]. This process results in the development of cross-links, rearrangement, and merging of cyclized sections, leading to a structural transition from a ladder structure to a graphite-like structure, and a morphological change from a smooth to a wrinkled surface. Carbonization can specifically eliminate non-carbonized volatile molecules such as $H_2O$, CO, HCN, $N_2$, $NH_3$, and $CO_2$. In addition, carbonization reduces the diameter of polymer fibers, resulting in a greater surface area and improved conductivity [10]. Carbon nanotubes (CNTs) are commonly employed as additives in electrospun fibers. They primarily serve as reinforcing elements in electrospun polymeric fibers, but they also adjust the electrical characteristics of the fibers by reducing their resistance to electricity flow. Furthermore, the presence of CNTs may facilitate the formation of carbon crystals as PAN undergoes carbonization [11, 12]. The study conducted by Ali and co-workers [1] revealed that incorporating MWCNTs enhanced the graphitic arrangement of PAN, they proposed an approach for producing CNFs developed with MWCNTs by fixing the edges of nanofiber mats and applying a constant creep stress throughout the stabilization process, they showed that applying creep stress results in enhanced graphitization compared to those without it. Stodolak-Zych et al. [13] found that adding a modest quantity of functionalized MWCNTs to the PAN significantly influences its stabilization process; moreover, the resulting CNFs containing CNTs display noticeably higher levels of organization compared to pure CNFs. While Zhang and his associates [3] demonstrated that

decreasing the diameter led to a higher degree of graphitization in CNF mats and produced more extensive cross-linking structures throughout the stabilization procedure. Zhou and his colleagues [6] reported that with an increase in the carbonization temperature to 2200 °C, CNFs exhibited a higher degree of graphitization and structural organization.
This study aims to synthesize carbon nanofibers (CNFs) with enhanced graphitization from electrospun PAN/CNT precursors through stabilization and carbonization processes at temperatures below 2000°C, a significant reduction compared to conventional methods using pure PAN precursors. Additionally, the impact of incorporating CNTs on the properties of the resulting CNFs was examined.

## 2. Materials and Methods

### 2.1 Materials

PAN supplied by Macklin, China with a molecular weight (Mw) of 150000 g/mol. Dimethylformamide (DMF ≥99%, Sigma Aldrich) was used as the solvent. Multi-walled carbon nanotubes (MWCNTs) purchased from Cheap Tubes Company, USA with a length of 10–30μm, outer diameter of 10–30 nm, and purity of 90% were used as reinforcement materials.

### 2.2 Preparation of the CNFs precursors

First, a 10% w/v PAN solution was prepared by dissolving PAN in DMF and stirring the mixture on a hot magnetic stirrer at 50 °C for 1 hour, resulting in a clear and homogeneous polymer solution. Next, a 10% w/v PAN/CNT solution was prepared by mixing the (MWCNTs: PAN) solution in a (1:9) ratio and magnetically stirring for 2 h [14, 15]. The mixture was then homogenized using ultrasonic waves (bath type) for 2 h to disperse the agglomerates and create a uniform black suspension. PAN and PAN/CNT nanofiber mats were fabricated using an electrospinning device (Bio-electrospinning/Electrospray System ESB-200, South Korea). The setup included a syringe containing the solution and a stainless-steel needle (inside diameter = 0.7 mm) as the nozzle, and the spinning parameters were set as follows: voltage, 20 kV; capillary collector distance, 20 cm; and feed rate, 1 mL/h.

### 2.3 Heat treatment

Before stabilization, the PAN and PAN/CNT precursors were placed in a specially designed alumina crucible (3.5×8.5×1.5 cm) to fix the membrane and prevent its movement and folding due to the flow of gas inside the furnace. This crucible was designed with an alumina breathable cover to keep the nanofiber precursor stable during heat treatment and, at the same time, allow the inert gas inside the crucible during carbonization, as shown in Figure 1.
For stabilization, the nanofiber mats were heated to 275 °C at a rate of 2 °C per minute and maintained at this temperature for 3 hours to ensure the completion of transformation. For carbonization, the stabilized nanofiber mats were heated at 1000 °C at a heating rate of 5 °C/min and held at this temperature for 1 h under an atmosphere of nitrogen flow of 5 mL/min. A tube furnace, GSL-1500X-50RTP (MTI Corporation, Richmond, USA), was used for both processes.

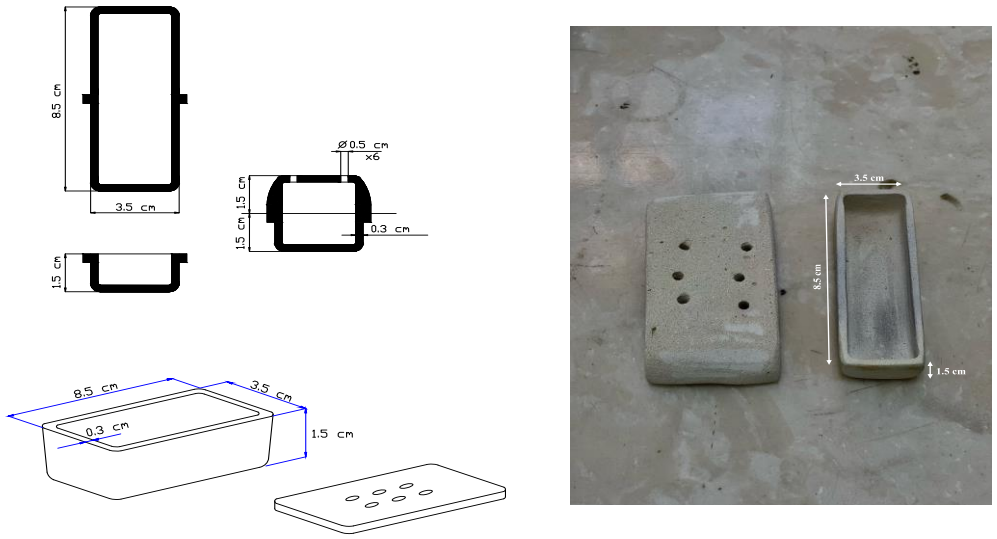


(a) (b)

**Figure 1:** (a) isometric and orthographic views of a rectangular crucible; and (b) a rectangular crucible with a breathable cover containing holes to allow permeabilizing gas into the membrane.

## 2.4 Characterization

Field emission scanning electron microscopy (FE-SEM) (Inspect TM F50) was employed to characterize the fiber morphology of the electrospun and carbonized nanofiber mats. The samples were coated with a thin layer of gold and examined by FE-SEM at an acceleration voltage of 5 kV. The diameters of 50 fibers from the FE-SEM images were measured using the ImageJ software. The average fiber diameter and standard deviation were estimated using Microsoft Excel [16]. The average percentage reduction in size (Sr%) of the carbonized fibers was computed by comparing their average diameter (dc) to the average diameter of the initial PAN fibers (dx) using Eq. (1) [17].

$$Sr\% = \left(\frac{dc - dx}{dx}\right) \times 100 \quad (1)$$

Fourier transform infrared (FTIR) spectroscopy (Bruker Optik system, Tensor 27, Germany) was used to characterize the chemical composition and capture the characteristic peaks of the electrospun and carbonized PAN and PAN/CNT nanofibers within the wavenumber range of 400–4000 $cm^{-1}$. Raman spectroscopy with an excitation laser wavelength of 532 nm (Bruker, Germany) was used to acquire data on the graphitic structure and defects in the carbonized PAN and PAN/CNT nanofibers. X-ray diffraction (XRD) analysis (Aeris Research Edition, Panalytical Company, Netherlands) was performed on the CNFs and CNF/CNT specimens by recording the 2θ angles in the range of 10° to 70° using Cu Kα radiation to understand the crystal phase of the prepared CNFs and CNFs/CNTs. To measure the electrical resistance R of the electrospun and carbonized PAN and PAN/CNT nanofiber mats using a Keithley Model 616 digital electrometer, a two-point electrode was made from silver paste. The electrical conductivity (σ) was determined using the Eq. (2) [6].

$$\sigma = \frac{L}{AR} \quad (2)$$

Where R is the electrical resistance of the nanofiber mats, A is the cross-sectional area of the nanofiber mats (with a square-shaped specimen geometry of 2×2 cm), and L is the distance between the two electrodes (1 cm) [6]. The measurements were conducted at room temperature of 25°C and relative humidity of 50%.

The water contact angle WCA of electrospun and carbonized PAN and PAN/CNT nanofibers was determined. The low-bond axisymmetric drop shape analysis LBADSA approach was utilized for measurement, and all WCA values were obtained by taking the average of seven measurements at various positions on the surface. A water droplet was carefully placed on the surface. The procedure was performed using a high-speed CCD camera set to capture 35 fps.

## 3. Results and Discussion

### 3.1 FE-SEM characterization

PAN precursor, PAN/CNT precursor, CNFs, and CNFs/ CNTs were characterized using FE-SEM, as shown in Figures 2 and 3, respectively. A drastic decrease was observed in the average fiber diameter from (176.2±69 nm) to (88.4±32 nm) after the addition of CNTs to pure PAN, as shown in Figures 2a-b. This reduction is related to the improved electrical conductivity of the PAN/ CNTs solution [14], which in turn increases fiber elongation during electrospinning, as demonstrated by Ali and co-workers [1]. As shown in Figure 3, both CNFs produced after heat treatment of PAN precursor and CNFs/CNTs produced after heat treatment of PAN/ CNTs precursor exhibited a decrease in the average fiber diameter, (132.06±82 nm) for CNFs and (76.43±4 nm) for CNFs/CNTs. Carbonization is carried out in an inert gas atmosphere, which specifically prevent oxidation and eliminates non-carbonized volatile molecules such as $H_2O$, CO, HCN, $N_2$, $NH_3$, and $CO_2$. This process results in the contraction of the fiber diameter and improved conductivity [10]. This reduction can be attributed to the evaporation of non-carbon elements during the stabilization and carbonization processes [1]. Furthermore, Carbonization caused a decrease in the fiber size across both assessed samples.

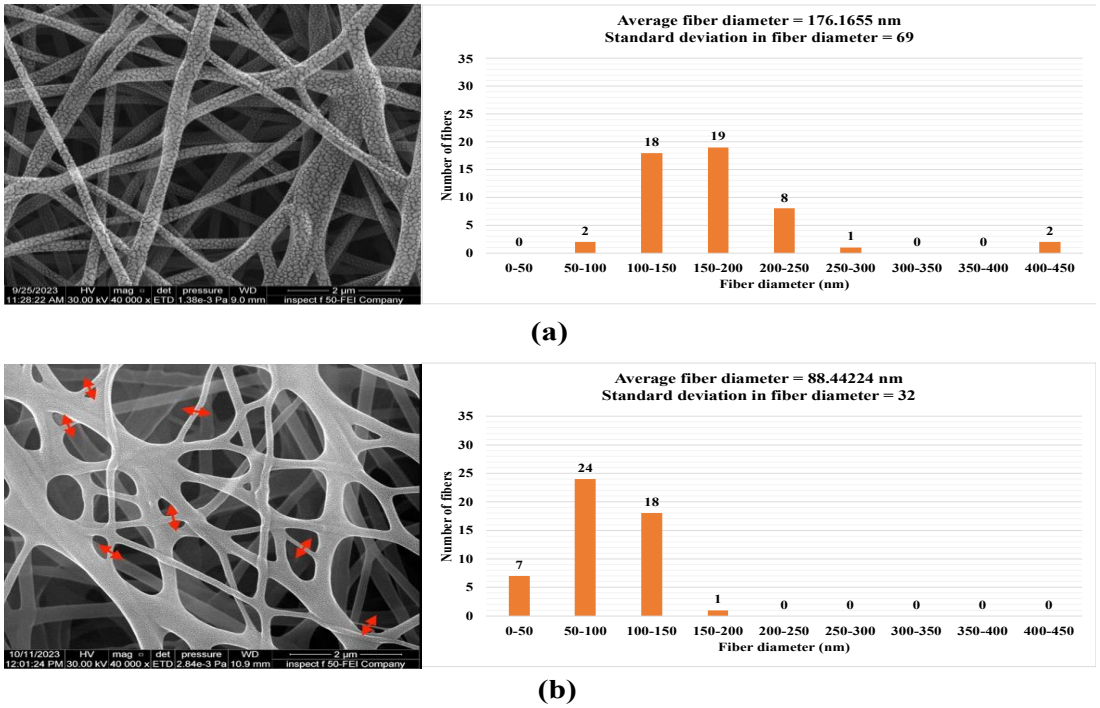


**Figure 2:** FE-SEM images (magnification of 40000×) and fiber diameter distribution of (a) PAN precursor and (b) PAN/CNTs precursor (Red arrows indicating the fibers with diameters ranging from 0-50 nm).

Significant reductions were observed in carbonized fibers compared to electrospun fibers: -25.05% for CNFs and -13.54% for CNFs/CNTs. The absence of CNTs results in the loss of

nearly half of the fiber diameter. The presence of CNTs led to a slightly smaller reduction in size, suggesting their potential involvement in the thermal stabilization process [17].

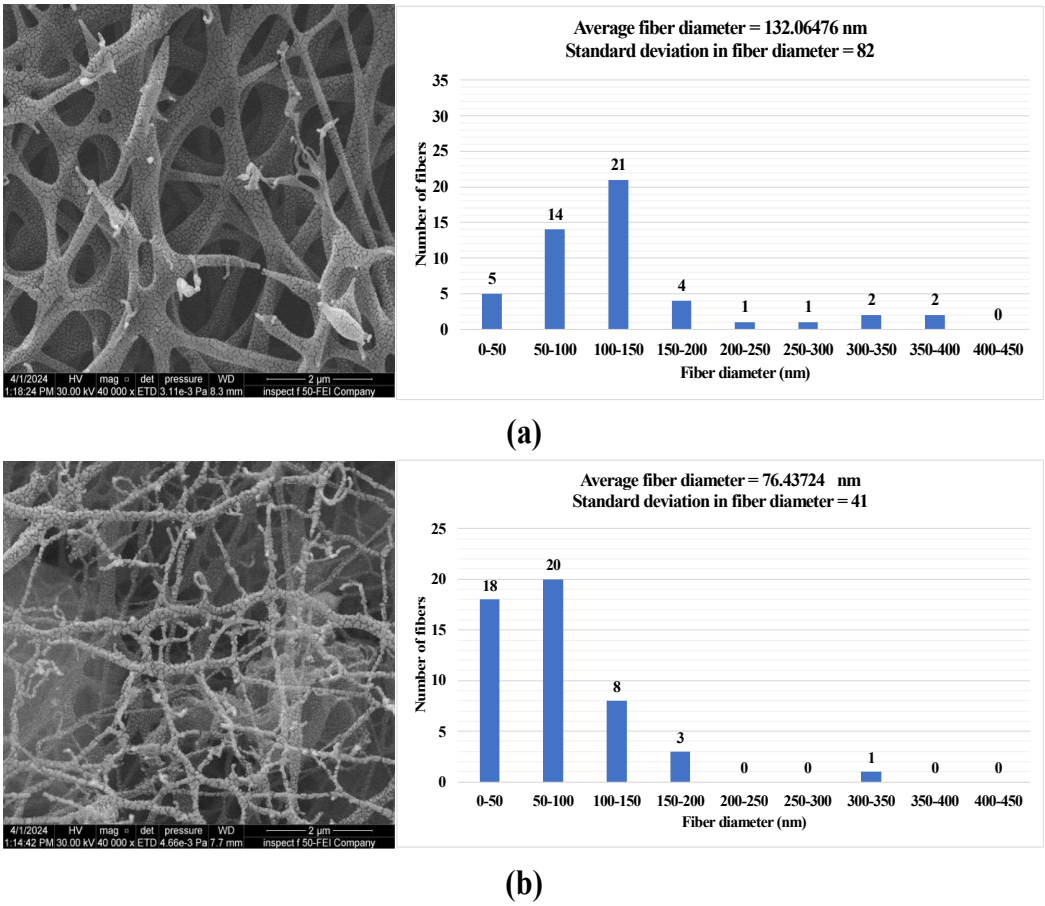


**Figure 3** FE-SEM images (magnification of 40000×) and fiber diameter distribution of (a) CNFs and (b) CNFs/CNTs after carbonization at 1000 °C.

### 3.2 Fourier transform infrared (FTIR) spectroscopy

Figures 4a-b show FTIR spectra of prepared specimens, identifying all the significant characteristic peaks. After stabilization, both PAN and PAN/CNT precursors experienced a remarkable change: a drastic decrease in the intensity of the nitrile group C≡N at 2242 $cm^{-1}$, accompanied by a peak evolution at 1541 $cm^{-1}$, arising from the existence of C=N and C=C bonds. This band is responsible for the creation of a ladder structure in PAN, which allows it to endure the high-temperature carbonization process without undergoing fusion. However, this peak had a higher intensity in the stabilized PAN/ CNTs sample, confirming the effectiveness of CNTs in C≡N transformation to C=N and C=C during stabilization, which is consistent with the findings reported by Liu [18].

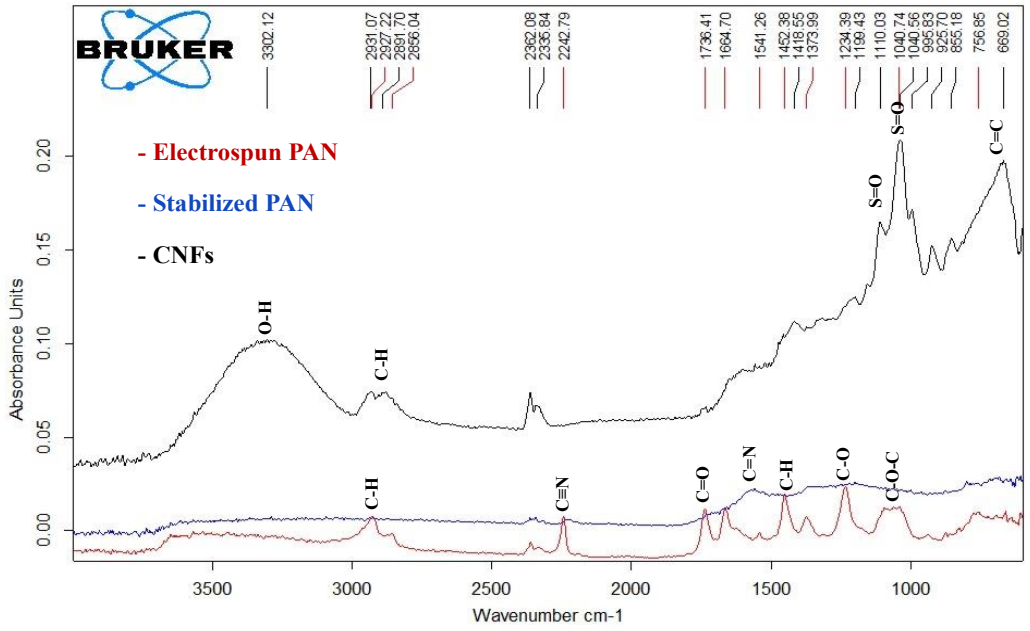


**(a)**

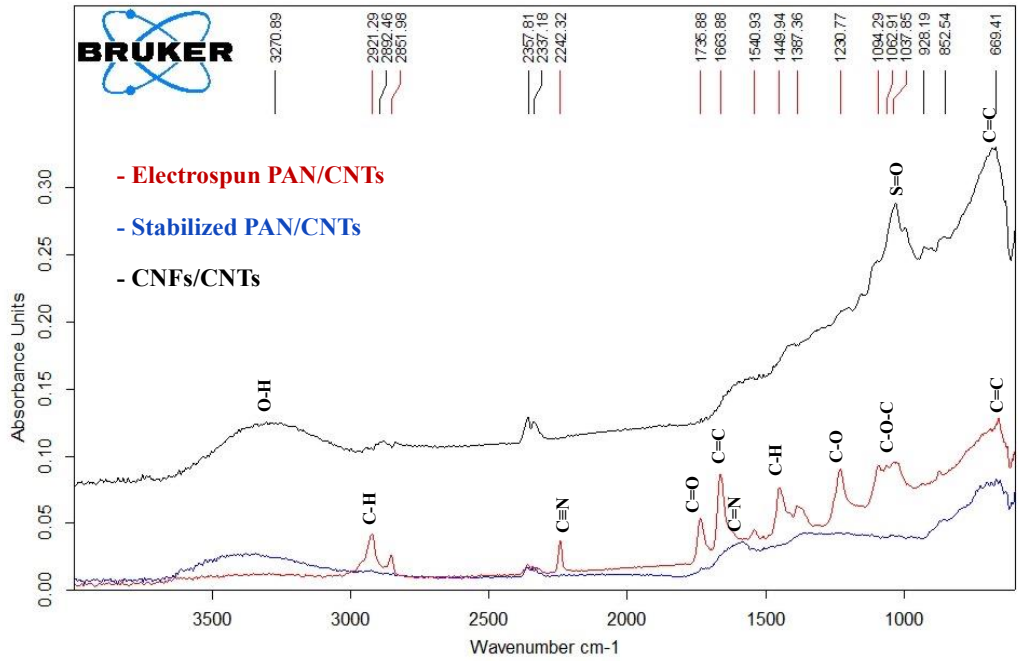


**(b)**

**Figure 4:** (a) FTIR spectra for electrospun PAN, stabilized PAN and CNFs; (b) FTIR spectra for electrospun PAN/CNTs, stabilized PAN/CNTs and CNFs/CNTs.

Furthermore, the presence of a distinct peak at 855 $cm^{-1}$ C=C-H, indicates that dehydrogenation has occurred [1]. After carbonization at 1000 °C, the materials produced no peaks associated with C≡N bonds, due to the structural transformation of PAN. During stabilization, C≡N bonds convert into C=N bonds, forming a ladder structure, which further rearranges into a graphite-like structure during carbonization, eliminating nitrogen-containing groups [8, 10].

A peak corresponding to the stretching of the saturated C-H bond at approximately 2879 $cm^{-1}$ was prominently observed in the CNFs and CNFs/CNT specimens. The peak at 1110

$cm^{-1}$ refers to lactones and/or esters, and the peak at 1031 $cm^{-1}$ is caused by the cyclization process, which induces CH deformation in monocyclic pyridine rings. The occurrence of PAN structure may be attributed to the residues of oxidation-reduction catalysts containing the S=O group. Moreover, both specimens exhibit a peak at 699 $cm^{-1}$, which is associated with the development of C=C bonds, but the intensity of this peak was higher in the CNFs/CNT specimen than in the CNFs specimen as a result of the presence of MWCNTs, which enhances the graphitization process [17, 19]. These results suggest that the absence of CNTs in the material reduces the effectiveness of graphitization and the structural arrangement of the sample induced by heat treatment.

### 3.3 X- Ray Diffraction XRD analysis and Raman spectroscopy

To confirm the phases and compositions of the prepared CNFs and CNFs/CNTs, they were examined using XRD. XRD curves of both specimens Figures 5a-b show the presence of two broad and weak peaks at 2θ values of 25–26° and 43°, which correspond to the (002) and (100) planes of graphite (JCPDS No. 75-1621), respectively [20, 21]. According to Musiol, this is normal because the growth of the crystallite sizes and subsequent decrease in the distance between the crystal lattice planes along the c-axis are only achieved when using high temperatures beyond 2000 °C [21]. However, the XRD patterns reveal the successful carbonization of CNFs and CNF/CNT specimens at 1000 °C, which is consistent with Zhang [22].

Raman spectroscopy was performed on both the CNFs and CNF/CNT specimens to determine the degree of graphitization after the addition of MWCNTs, as shown in Figure 5c. The two main bands, the D-band at 1350 cm-1 refers to defects and disorder in the graphitic structure, While the G-band at 1590 cm-1 refers to the radial stretching of $sp^2$ carbon atoms in the C-C bond and is evidence of highly ordered carbon structures. A higher R ratio or $I_D/I_G$ Intensity ratio indicates the existence of flaws within the carbon layers, whereas a lower $I_D/I_G$ ratio indicates the degree of structurally organized graphite crystallites present in carbonaceous materials [6, 23]. For CNFs/CNTs, the $I_D/I_G$ ratio decreases slightly from 1.22 for CNFs to 1.15 for CNFs/CNTs, indicating that the addition of CNTs can enhance the crystallinity of the fibers and transform disordered carbonaceous components into more organized graphite crystallites [1]. In addition, according to Stodolak-Zych, CNTs act as catalysts in both the cyclization and graphitization processes of CNFs. CNTs may act as heterogeneous nuclei for graphitization, potentially enhancing the polymer's crystalline structure during heat exposure. This led to an increase in the G-band, which became sharper in the CNF/CNT specimen [13].

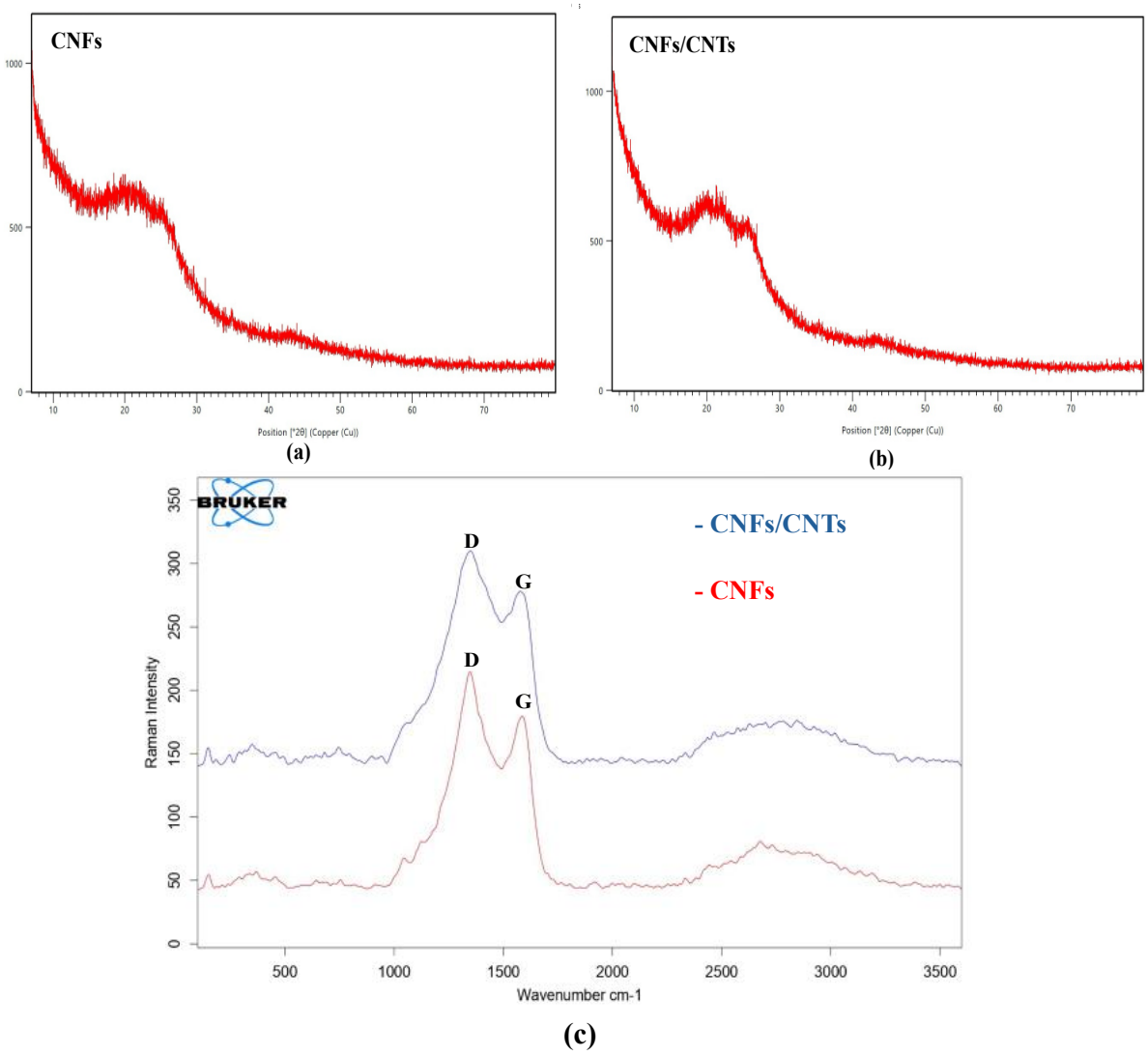


**Figure 5:** (a) XRD patterns of CNFs; (b) XRD pattern of CNFs/CNTs; and (c) Raman spectra for CNFs and CNFs/CNTs specimens.

### 3.4 Electrical conductivity (EC) test

EC of CNFs and CNFs/CNTs were compared with those of PAN and PAN/CNT precursors. Pure PAN precursors exhibited a negligible conductivity around 2.27×10-11 S/cm; after the addition of MWCNTs, it increased to 0.7 S/cm in the PAN/CNTs. This may be attributed to the high electrical conductivity of CNTs and the increased entanglement and contact between nanofibers after the addition of MWCNTs, which is consistent with Zhou, who also proved that increasing the entanglement and contact between nanofibers increases the electrical conductivity [6]. After carbonization, the EC of CNFs was 0.8 S/cm, while CNFs/CNTs resulted in higher conductivity up to 1.9 S/cm compared to CNFs alone.

The presence of CNTs leads to enhanced charge transport by creating a medium for conduction, enabling the movement of electrons within the composite structure of the fibers, which in turn increases electrical conductivity [24]. In general, the enhancement in electrical conductivity indicates that the structure becomes more graphitic and ordered [6].

### 3.5 Water contact angle (WCA) test

As shown in Figure 6, WCA values for PAN precursor, PAN/CNT precursor, CNFs, and CNFs/CNTs were 140±2°, 45±2°, 40±2°, and 18±2°, respectively. A WCA assessment was performed to evaluate the wettability of the electrospun and carbonized specimens. Because the WCA of the PAN precursor has a value of $90° < \theta < 150°$, it is considered hydrophobic. The WCA for the other specimens had values of $0° < \theta < 90°$; therefore, they were considered hydrophilic [25]. The addition of CNTs, stabilization, and carbonization treatments decreased the WCA, indicating an enhancement in surface hydrophilicity (wettability of the CNFs).

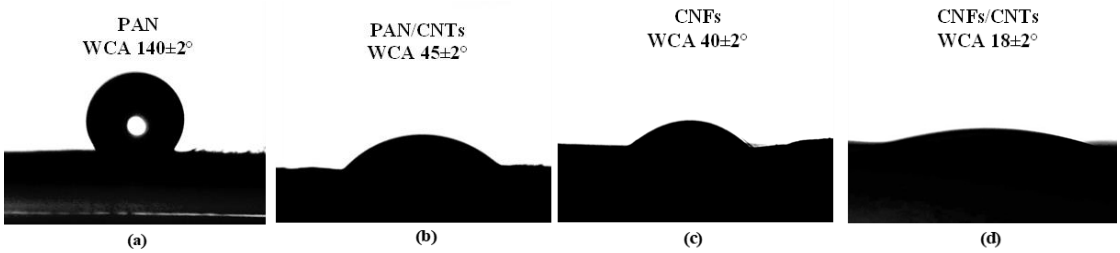


**Figure 6:** WCA measurement for (a) PAN precursor, (b) PAN/CNTs precursor, (c) CNFs and (d) CNFs/CNTs.

## Conclusions

In summary, modified CNFs/CNTs were successfully synthesized from PAN/CNTs electrospun precursors, followed by stabilization at 275°C and carbonization at 1000°C. The addition of MWCNTs maintained the fibers with a lower average percentage reduction in size Sr% after carbonization compared with traditional CNFs. FTIR spectroscopy and XRD analysis confirmed the effectiveness of the heat treatment used to transform PAN and PAN/CNT precursors to CNFs and modified CNFs/CNTs, respectively. Raman spectroscopy showed the improved graphitization in CNFs/CNTs by the decrease in $I_D/I_G$ intensity ratio from 1.22 for CNFs to 1.15 for CNFs/CNTs which means yielding more organized graphite crystals. The electrical conductivity of the modified CNFs/CNTs was also enhanced compared to that of the traditional CNFs. The wettability of traditional CNFs was enhanced by the addition of MWCNTs. The lowest water contact angle WCA was recorded for the CNF/CNT specimen (18±2°). This indicates the effectiveness of the modified CNFs/CNTs in many applications that require hydrophilicity, such as tissue-engineering applications. Further research should be conducted to synthesize modified CNFs by adding other ceramic and metallic reinforcements and carbonization at temperatures higher than 1000 °C.

## Acknowledgements

This research was supported by the Department of Materials Engineering, University of Technology, Iraq.

## Ethics Statement

This article does not contain any studies involving animals performed by any of the authors.

## Conflict of interest

The authors declare that they have no competing interests.

**References**


**[1]** A. B. Ali, D. Slawig, A. Schlosser, J. Koch, N. C. Bigall, F. Renz, C. Tegenkamp, R. Sindelar, "Polyacrylonitrile (PAN) based electrospun carbon nanofibers (ECNFs): Probing the synergistic effects of creep assisted stabilization and CNTs addition on graphitization and low dimensional electrical transport," *Carbon*, vol. 172, pp. 283–295, 2021. https://doi.org/10.1016/j.carbon.2020.10.033

**[2]** X. Zhou, Y. Wang, C. Gong, B. Liu, and G. Wei, "Production, structural design, functional control, and broad applications of carbon nanofiber-based nanomaterials: A comprehensive review," *Chemical Engineering Journal*, vol. 402, p. 126189, 2020. https://doi.org/10.1016/j.cej.2020.126189

**[3]** W. Zhang, Q. Sun, Z. Shen, J. Liu, and X. Wang, "Effect of Diameter on the Structural Evolution and Tensile Properties of Electrospun PAN-Based Carbon Nanofiber Mats," *ACS Omega*, *vol. 8*, no. 21, pp.19002-19005, 2023. https://doi.org/10.1021/acsomega.3c01708

**[4]** C. Liu, K. Lai, W. Liu, M. Yao, and R. Sun, "Preparation of carbon nanofibres through electrospinning and thermal treatment," *Polymer International*, vol. 58, no. 12, pp. 1341–1349, 2009. https://doi.org/10.1002/pi.2669

**[5]** A. H. Oleiwi, A. R. Jabur, and Q. F. Alsalhy, "Polystyrene/Mwcnts nanofiber membranes characterizations in reducing sulfur content in crude oil," *Key engineering materials*, vol. 886, pp. 86–96, 2021. https://doi.org/10.4028/www.scientific.net/KEM.886.86

**[6]** Z. Zhou, C. Lai, L. Zhang, Y. Qian, H. Hou, D.H. Reneker, H. Fong, "Development of carbon nanofibers from aligned electrospun polyacrylonitrile nanofiber bundles and characterization of their microstructural, electrical, and mechanical properties," *Polymer*, vol. 50, no. 13, pp. 2999–3006, 2009. https://doi.org/10.1016/j.polymer.2009.04.058

**[7]** R. Schierholz, D. Kröger, H. Weinrich, M. Gehring, H. Tempel, H. Kungl, J. Mayer, R.A. Eichel, "The carbonization of polyacrylonitrile-derived electrospun carbon nanofibers studied by in situ transmission electron microscopy," *RSC Advances*, vol. 9, no. 11, pp. 6267–6277, 2019. https://doi.org/10.1039/C8RA10491C

**[8]** A. Mataram, A. F. Ismail, M. S. Abdullah, B. C. Ng, and T. Matsuura, "A review of assembled polyacrylonitrile-based carbon nanofiber prepared electrospinning process," *International Journal of Nanoscience*, vol. 10, no. 03, pp. 455–469, 2011. https://doi.org/10.1142/S0219581X11008228

**[9]** T. D. Nguyen and J. S. Lee, "Electrospinning-based carbon nanofibers for energy and sensor applications," *Applied Sciences*, vol. 12, no. 12, p. 6048, 2022. https://doi.org/10.3390/app12126048

**[10]** S. Peng, L. Li, J.K. Lee, L. Tian, M. Srinivasan, S. Adams, S. Ramakrishna, "Electrospun carbon nanofibers and their hybrid composites as advanced materials for energy conversion and storage," *Nano Energy*, vol. 22, pp. 361–395, 2016. https://doi.org/10.1016/j.nanoen.2016.02.001

**[11]** P. Heikkilä et al., "Preparation of electrospun PAN/CNT composite fibres," *in 17th International Conference on Composite Materials*, ICCM-17, Edinburgh, UK, 2009, pp. 1-7

**[12]** A. R. Jabur, F. A. Chayad, and N. M. Jalal, "Fabrication and characterization of nylon 6/MWCNTs conductive polymer by electrospinning technique," *International Journal of Thin Films Science and Technology*, vol. 5, no. 2, pp. 1–9, 2016. https://dx.doi.org/10.18576/ijtfst/050205

**[13]** E. Stodolak-Zych, A. Benko, P. Szatkowski, E. Długoń, M. Nocuń, C. Paluszkiewicz, M. Błażewicz, "Spectroscopic studies of the influence of CNTs on the thermal conversion of PAN fibrous membranes to carbon nanofibers," *Journal of Molecular Structure*, vol. 1126, pp. 94–102, 2016. https://doi.org/10.1016/j.molstruc.2016.01.022

**[14]** F. M. Yahya, M. A. Najim, M. S. Hamza, "Polymer concentration adjustment for homogeneous carbon nanofibers precursors," *Physica Scripta*, vol. 99, no. 10, 2024. https://iopscience.iop.org/article/10.1088/1402-4896/ad7ae0/meta

**[15]** A. H. Oleiwi, A. R. Jabur, and Q. F. Alsalhy, "Morphology of polystyrene nano-fiber membranes reinforced with copper oxide and zirconium oxide nanoparticles as a sulfur absorbent material," *in AIP Conference Proceedings, AIP Publishing*, vol. 2769, no. 1, 2023. https://doi.org/10.1063/5.0129144

**[16]** M. A. Najim, B. I. Khalil, and A. A. Hameed, "Characterizing optimum electrospinning conditions for graft urethanized Poly (Vinyl Alcohol) (U-PVA)," *Heliyon,* vol. 8, no. 11, 2022. https://doi.org/10.1016/j.heliyon.2022.e11423

**[17]** A. Benko, M. Nocuń, M. Gajewska, and M. Błażewicz, "Addition of carbon nanotubes to electrospun polyacrylonitrile as a way to obtain carbon nanofibers with desired properties," *Polymer Degradation and Stability*, vol. 161, pp. 260–276, 2019. https://doi.org/10.1016/j.polymdegradstab.2019.01.033

**[18]** Y. Liu, "Stabilization and carbonization studies of polyacrylonitrile/carbon nanotuanotube composite fibers," Ph.D. dissertation, School of Materials Science and Engineering, Georgia Inst. Technol., Atlanta, GA, USA, 2010.

**[19]** J. C. Simitzis and P. C. Georgiou, "Functional group changes of polyacrylonitrile fibres during their oxidative, carbonization and electrochemical treatment," *Journal of Materials Science*, vol. 50, no. 13, pp. 4547–4564, 2015. https://doi.org/10.1007/s10853-015-9004-2

**[20]** H. Samadian, H. Mobasheri, S. Hasanpour, J. Ai, M. Azamie, and R. Faridi-Majidi, "Electro-conductive carbon nanofibers as the promising interfacial biomaterials for bone tissue engineering," *Journal of Materials Science*, vol. 298, p. 112021, 2020. https://doi.org/10.1016/j.molliq.2019.112021

**[21]** P. Musiol, P. Szatkowski, M. Gubernat, A. Weselucha-Birczynska, and S. Blazewicz, "Comparative study of the structure and microstructure of PAN-based nano-and micro-carbon fibers," *Ceramics International*, vol. 42, no. 10, pp. 11603–11610, 2016. https://doi.org/10.1016/j.ceramint.2016.04.055

**[22]** Z. Zhang, X. Deng, J. Sunarso, R. Cai, S. Chu, J. Miao, W. Zhou, Z. Shao, "Two-step fabrication of Li4Ti5O12-coated carbon nanofibers as a flexible film electrode for high-power lithium-ion batteries," *ChemElectroChem*, vol. 4, no. 9, pp. 2286–2292, 2017. https://doi.org/10.1002/celc.201700351

**[23]** J. Markowski, M. Zambrzycki, W. Smolka, A. Panek, M. Gubernat, P. Czaja, M. Marzec, A. Fraczek-Szczypta, "Influence of Heat Treatment of Electrospun Carbon Nanofibers on Biological Response," *International Journal of Molecular Sciences*, vol. 23, no. 11, p. 6278, 2022. https://doi.org/10.3390/ijms23116278

**[24]** F. A. Chayad, A. R. Jabur, and N. M. Jalal, "Effect of MWCNT addition on improving the electrical conductivity and activation energy of electrospun nylon films," *Karbala International Journal of Modern Science*, vol. 1, no. 4, pp. 187–193, 2015. https://doi.org/10.1016/j.kijoms.2015.10.004

**[25]** D. Quéré, "Wetting and roughness," *Annual Review of Materials Research*, vol. 38, pp. 71–99, 2008. https://doi.org/10.1146/annurev.matsci.38.060407.132434